J. Cent. South Univ. Technol. (2008) 15: 69−74
DOI: 10.1007/s11771−008−0015−x

Springer

Influence of underground water seepage flow on surrounding rock deformation of multi-arch tunnel

LI Xi-bing(李夕兵)[1,2], ZHANG Wei(张 伟)[1], LI Di-yuan(李地元)[1,2], WANG Qi-sheng(王其胜)[1,3]

(1. School of Resources and Safety Engineering, Central South University, Changsha 410083, China;
2. Hunan Key Laboratory of Resources Exploitation and Hazard Control for Deep Metal Mines, Changsha 410083, China;
3. School of Energy Sources Engineering, Henan Polytechnic University, Jiaozuo 454150, China)

Abstract: Based on a typical multi-arch tunnel in a freeway, the fast Lagrangian analysis of continua in 3 dimensions($FLAC^{3D}$) was used to calculate the surrounding rock deformation of the tunnel under which the effect of underground water seepage flow was taken into account or not. The distribution of displacement field around the multi-arch tunnel, which is influenced by the seepage field, was gained. The result indicates that the settlement values of the vault derived from coupling analysis are bigger when considering the seepage flow effect than that not considering. Through the contrast of arch subsidence quantities calculated by two kinds of computation situations, and the comparison between the calculated and measured value of tunnel vault settlement, it is found that the calculated value(5.7−6.0 mm) derived from considering the seepage effect is more close to the measured value(5.8−6.8 mm). Therefore, it is quite necessary to consider the seepage flow effect of the underground water in aquiferous stratum for multi-arch tunnel design.

key words: multi-arch tunnel; underground water seepage flow; coupling flow and stress; surrounding rock deformation; vault settlement

1 Introduction

With high speed development of our national economy, the highway is constructed on large-scale all around the country. Along the freeway from Changsha to Chongqing(one section of which is from Changde to Jishou), many tunnels have to be constructed. As these tunnels's topography and geomorphic conditions are very complex and the rain is very rich, the invasion of underground water and surface water is a difficult problem in the tunnel construction and its future function. In the past railway and highway tunnel construction, some effective waterproof construction technologies were proposed[1−3]. But the researches on the mechanism of coupling function of fluid and stress and its influence on tunnels are not enough. For example, LIU and CHEN[4] calculated and analyzed the double-arch tunnel structure in water-eroded groove but did not consider the underground water seepage force. YANG et al[5] studied the earthquake response of large span and double-arch shallow tunnel, combining with dynamic stress but without underground water seepage stress. In fact, tunnel excavation forms two secondary stresses fields that can change the distribution of initial rock stress field and the underground water seepage field. And the seepage flow of underground water also has important influence on the stability of tunnel.

Generally speaking, when the surface water seeps in underground, it will constitute the initial seepage flow field together with the underground water. But after tunnel excavation the initial seepage flow field will be destructed. In order to achieve a new balance, it can produce a new seepage flow field around the tunnel with the underground water flowing into the tunnel. The pore-water pressure can change the stress field of adjacent rock mass. This problem is the coupling flow and stress question on which some scholars study now[6−9]. LI et al[6] analyzed the subsea tunnel with coupling process and LEE and NAM[8−9] discussed the seepage flow force around the tunnel with coupling analysis. In order to know the effect of underground water seepage flow on the surrounding rock deformation of tunnel, a multi-arch tunnel(named Bi-Ma-Xi tunnel) engineering was analyzed with $FLAC^{3D}$ in this work.

2 Engineering and geology conditions

2.1 Topography

The tunnel locates at a hill on long-term weathering and denudation action. In the tunnel area, there are some gullies that primarily strike towards north and some

Foundation item: Project(50490274) supported by the National Natural Science Foundation of China; Project(200516) supported by Hunan Transportation Science and Technology
Received date: 2007−05−21; **Accepted date**: 2007−07−21
Corresponding author: LI Xi-bing, PhD, Professor; Tel: +86−731−8879612; E-mail: xbli@mail.csu.edu.cn

strike from east to north. Tunnel axis direction and topographic contour line are intersected with orthogonal or a great angle at section K218+087−K218+380 and with a small angle or even parallel at section K218+380−K218+565. The topography is rather steep and forms a "V" type gully. The general hill strike is about 340°, which is close from north to south. The topography slope is about 15°−35°. The green vegetation is mainly the small bamboo and herbaceous plants. The rock bed is visible in some places.

2.2 Lithology

According to engineering geology survey and drilling exposure data, the stratum of surveying area from young to old is as follows.

The Quaternary Holocene(Qh): the soil-like loam layer, snuff color, plastic-stiffly, 0−4.60 m thick. This layer is ignored in numerical model.

The Upper Cretaceous (K2j): Sandstone layer, red brown or palm fibre or dust colour, fine-grained structure. The calcareous cemented rock layer is mixed with mud cemented rock layer and the former is the main part and it is thin and medium thickness structural layer. The horizontal bedding layer develops and the dip angle is small. According to weathered degree the stratum can be divided into three layers from the top down: intensely, weakly and tinily weathered layer. The sketch map of geology section is shown in Fig.1.

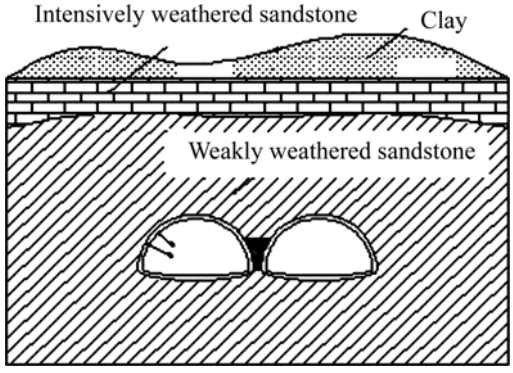

Fig.1 Sketch of geological profile for tunnel

2.3 Geology constitution

In tunnel area there is no large fracture structure and nor any new tectogenesis. The geology constitution is a monoclinal structure. The rock dip direction of general occurrence is 95°−115°. The dip angle distribution ranges from 8° to 15°. Three sets of joint crack develop: 1) dip direction 148°, dip angle 89°; 2) dip direction 350°, dip angle 56°; 3) dip direction 225°, dip angle 77°. The joint cracks mostly twist with pressure and crack faces are almost close. Minorities of the crack faces are patulous and the distance between two cracks often varies from 5 to 20 cm. The connectivity is fairly good.

3 Construction of 3D numerical model

3.1 model of numerical calculation

This tunnel is a freeway multi-arch tunnel, of which the left one and right one are general parallel. The two tunnels are about symmetrical by the middle arch wall. The average thickness of middle wall is 2.1 m. The key dimensions of tunnel section are shown in Fig.2.

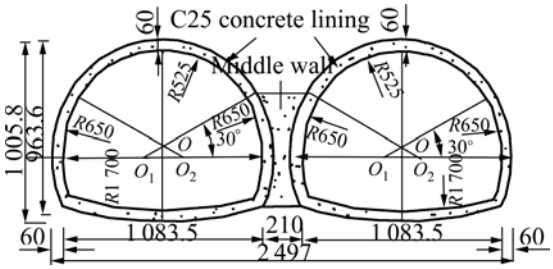

Fig.2 Sketch of multi-tunnel cross section (unit: cm)

When modeling the tunnel, the direction along the tunnel is *y*-axis and in horizontal plane the perpendicularity of tunnel direction is *x*-axis and plumb upward is z-axis. The influence of tunnel excavation is considered. The radius of influence range is above 3 times of one tunnel span. So in width direction, 50 m extends respectively outside the left and right tunnel, plus the span itself, width direction calculation range is 125 m. Downwards from the original point is 3 times of the height of the tunnel, which equals 45 m and upward is till the earth's surface (does not consider the clay layer, calculating depth range includes intensely, weakly, tinily weathered red sandstone from above to below respectively). The buried depth of the tunnel is about 25 m. Plus the 10 m of its height, in *z*-axis the depth is 80 m. Along the tunnel direction an unit length is considered because tunnel excavation can be considered as a plane-strain problem. The size of the 3D numerical model is 125 m×80 m×1 m. The 3D numerical model and its coordinate axis location are shown in Fig.3.

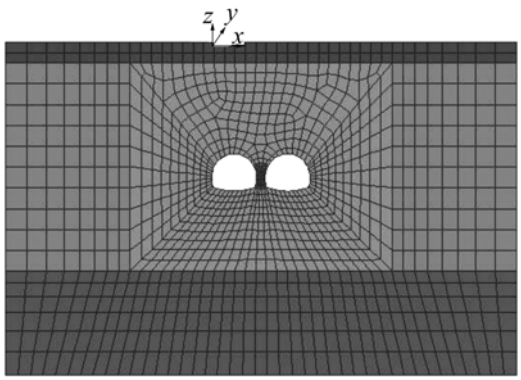

Fig.3 3D numerical model of tunnel in FLAC^{3D}

The displacement boundary conditions are adopted in numerical model. Bottom border is constrained with vertical displacement and upper border is free border. Both left and right border are restrained with horizontal displacement. The same boundary conditions are applied in both the front and back borders in *y*-axis.

3.2 Calculation parameters

The mechanics parameters in numerical analysis are provided by geotechnical engineering investigation data and combined with the national criterion need and parameters discount request in numerical simulation. The mechanics parameters of the surrounding rock and the C25 concrete middle arch wall are listed in Table 1. The surrounding rock and the concrete intensity criteria adopted is the elastic-plastic criterion of Mohr-Coulomb. Table 2 shows the surrounding rock relevant seepage flow parameters when coupling problem is considered in numerical simulation. Table 3 lists the parameters of shot concrete(primary lining) and anchor support structure of the multi-arch tunnel. In this calculation process, the parameters of Grade IV surrounding rock supporting system are adopted. And only the affection of the anchor and shotconcrete is considered. The effect of secondary lining is not considered in numerical simulation.

4 Discussion on calculation results

4.1 Surrounding rock deformation characteristics without underground water seepage flow

Based on the established numerical model, the process in which the underground water seepage flow function was not considered was carried on by FLAC^{3D}. Fig.4 shows the vertical displacement contour-line map in this instance after multi-arch tunnel excavation. From Fig.4 it can be obviously seen that nearby the tunnel excavation region the rock deformation is relatively serious. The vault rock displacement is negative, indicating that the displacement direction is vertical downwards and subsidence occurs. But around the tunnel bottom the surrounding rock displacement is positive, indicating that the direction is vertical upwards and bulging phenomenon occurs.

In the process of numerical calculation, the left and right tunnels were simulated simultaneously, namely they were excavated in the identical section plane simultaneously, that is to say, the influence of the construction order is not considered. In the computation process of FLAC^{3D}, some interesting grid points were selected to monitor their vertical displacement. The monitored grid points' number and corresponding coordinate position are listed in Table 4.

Table 1 Mechanics parameters of surrounding rock(red sandstone) and middle wall in numerical analysis

Weathered condition of red sandstone	Elastic modulus/GPa	Poisson ratio	Friction angle/(°)	Density/ (kN·m^{-3})	Cohesion stress/MPa	Tensile stress/MPa	Depth/ m
Intensely weathered	0.1	0.45	30	20.0	0.1	0.07	5
Weakly weathered	0.5	0.30	40	22.0	0.4	0.3	50
Tinily weathered	2.0	0.20	48	24.0	1.5	1.2	25
C25 concrete	28.0	0.20	50	27.0	6.0	1.3	

Table2 Calculation parameters of underground water seepage flow in coupling analysis by FLAC^{3D}

Location	Lithology of sandstone	Nature porosity ratio	Infiltration coefficient/(cm·s^{-1})	Porosity ratio	Infiltration ratio/ (m^2·Pa^{-1}·s^{-1})
Bi-Ma-Xi tunnel K218+120-K 218+135	Intensively weathered	0.82	1.23×10^{-3}	0.45	1.23×10^{-9}
	Weakly weathered	0.67	4.70×10^{-4}	0.40	4.70×10^{-10}
	Tinily weathered	0.33	3.06×10^{-5}	0.25	3.06×10^{-11}
	Disturbed area	0.79	4.10×10^{-3}	0.44	4.10×10^{-9}

Note: porosity ratio $n=e/(1+e)$, e means nature porosity; Infiltration ratio $k=k_H g(g\rho_W)^{-1}$, g means acceleration of gravity, which is considered as 10 m/s^2, ρ_W means the density of underground water, which equals 1 000 kg/m^3.

Table 3 Design parameters of support structure

Grade of surrounding rock	Anchor	Shot concrete	18# I steel
V	HBC22N combination anchor, L = 3.0 m, row space: 1.00 m×0.75 m	C20: thick 26 cm	Space: 75 cm
IV	20MnSi common slurry anchor, L = 3.0 m, row space: 1.20 m×1.00 m	C20: thick 20 cm	
III	20MnSi common slurry anchor, L = 2.5 m, row space: 1.20 m×1.00 m	C20: thick 10 cm	

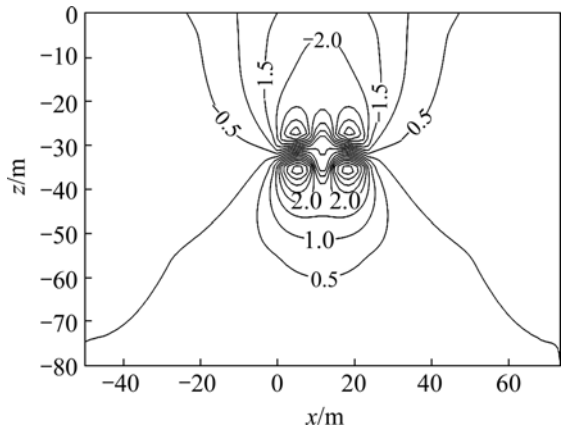

Fig.4 *z*-displacement contour-line map of surrounding rock without considering underground water seepage flow function (unit: mm)

Table 4 Monitored grid point's position of surrounding rock around tunnel's vault

Sequence	Coordinate location/m	Grid point number
1	3.9, 0, −26.9	41#
2	3.4, 0, −20.9	150#
3	4.0, 0, −14.2	209#
4	5.2, 0, −7.0	110#

Fig.5 shows the time process curves of *z*-displacement (absolute value) of the monitored grid points around left tunnel vault. From Fig.5 it can be seen that the vertical displacement value(or called settlement value) of tunnel vault surrounding rock has relationship with its own position. The closer the grid point's position away from the tunnel excavation region, the larger the settlement value. For example, on the middle upper grid point (41#) of left tunnel, its final calculation settlement value is 3.7 mm, and another grid points' values are getting smaller with the distance becoming longer.

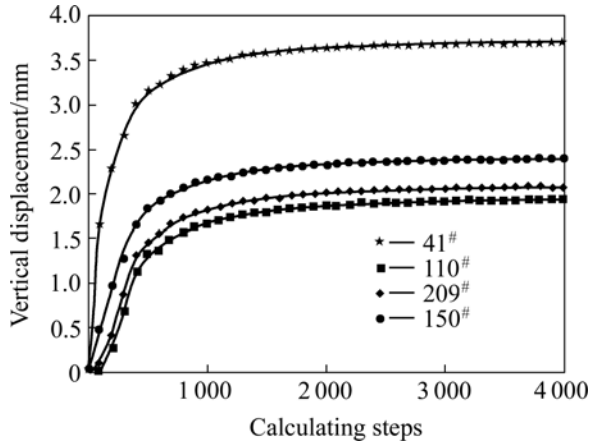

Fig.5 Time process curves of *z*-displacement of monitored grid points around left tunnel vault

4.2 Surrounding rock deformation characteristics with underground water seepage flow

The influencing factors of surrounding rock deformation after tunnel excavation in Refs.[10−13], mainly concentrating on the grade of surrounding rock, excavating and supporting method, the neighbor construction load and the construction working procedure. Generally it almost does not consider the influence of underground water seepage flow. But in fact, the underground water existence has important influence on the surrounding rock deformation. For instance, in the excavation and tunnel engineering, the underground water seepage flow can cause quite big displacement of the soil or rock mass and even threaten the safety of engineering[14−15]. In this study, some quantitative researches on the influence of surrounding rock deformation were carried out by underground water seepage flow.

The stratum is fully saturated with water before tunnel is excavated. The seepage flow boundary condition includes that the pore-water pressure of the top surface is limited to zero and the two sides as well as the base boundary are water-proof boundaries[16]. Before tunnel excavation the pore pressure of the stratum is hydro-static pressure. After tunnel excavation, around the tunnel excavation boundary is simulated by a free water seepage flow boundary where the adjacent underground water infiltrates into the excavated area. And the seepage flow field of surrounding rock has been changed with the excavation being carried on. Then the coupling analysis was executed by FLAC3D.

Fig.6 shows the vertical displacement contour-line map after multi-arch tunnel excavation when considering the underground water seepage flow function. Obviously it can be seen that in coupling analysis the arch subsidence quantity is larger than that of not considering seepage function and the affected region is also wider than that of the former as shown in Fig.4.

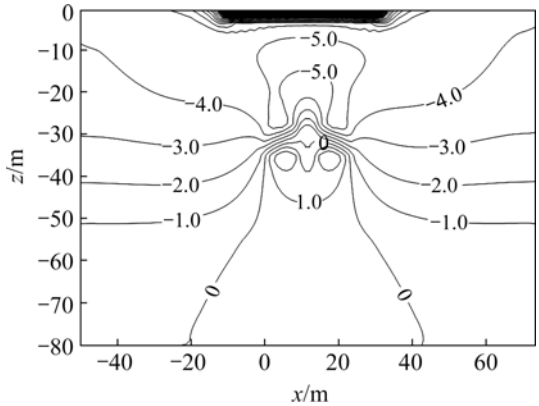

Fig.6 *z*-displacement contour-line map of surrounding rock when considering underground water seepage flow function (unit: mm)

In coupling analysis, as the change of pore pressure in surrounding rock, the effective stress will be changed and it will cause the rock porosity ratio to reduce, leading to a larger arch subsidence quantity compared with that of not considering the seepage flow effect. But the vertical displacements at the bottom of the tunnel are not changed a lot. Fig.7 shows the calculated vertical displacement value for both vault's middle position (grid point $41^{\#}$ and grid point $52^{\#}$). It can be seen that the subsidence quantity gradually increases with computation development, after finally tends to its new balance, both vault's vertical displacement quantities finally stabilize at about 5.7 mm and the two time process curves are basically consistent.

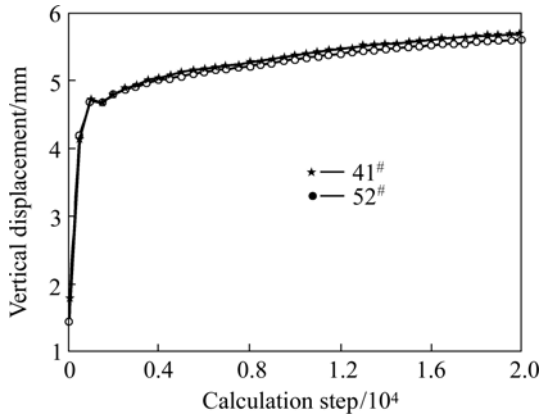

Fig.7 Curves of both vault's node displacement vs calculation steps

Fig.8 shows the time process curves of *z*-displacement (absolute value) of the monitored grid points around the left tunnel vault when taking the underground water seepage flow into consideration. Contrasting with Fig.5 it is obviously seen that the settlement value of $41^{\#}$ grid point is increased and reaches 5.7 mm. And to the other monitored grid points, their subsidence quantities also basically tend to 5.0 mm. The calculation subsidence quantities do not change when their relative positions changes.

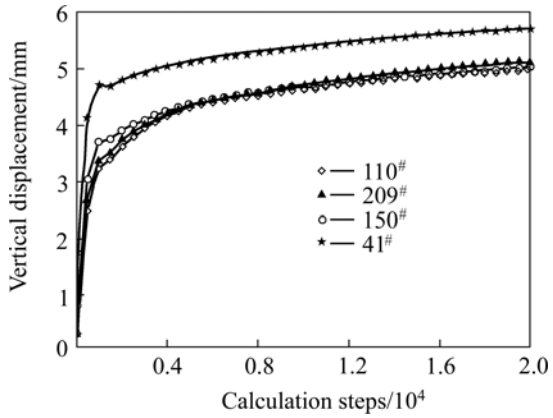

Fig.8 Time process curves of vault settlement when taking underground water seepage flow into consideration

4.3 Comparison of deformation measurement results of surrounding rock

In the process of excavating, the Bi Ma-Xi tunnel, the inspecting and consulting company of the fourth investigation and design institute of Chinese Railways Ministry monitored the surrounding rock deformation. Fig.9 shows the monitored vault settlement curves at sections K218+280 and K218+310.

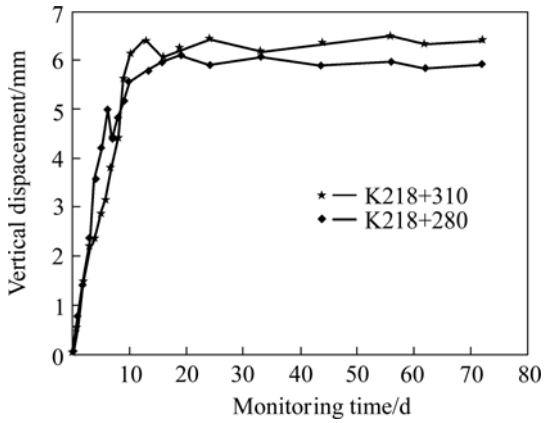

Fig.9 Curves of measured value of vault settlement in process of left tunnel excavation

Comparing Fig.9 with Fig.5 and Fig.8, the maximal vault settlement calculation value is 3.7 mm when without considering underground water seepage flow, and when taking it into consideration the maximal calculation value is equal to 5.7 mm. And the practical monitored results reach 6.5 mm and tend to be stable after 2 months when the tunnel is excavated. The case fits very well with the coupling analysis result. The vault settlement measurement values in this multi-arch tunnel are all basically leveled off between 5.8 mm and 6.8 mm.

The calculation results of coupling fluid-mechanical analysis are slightly smaller than the measured results. The reason is that the numerical calculation is thought as converged when the maximal unbalanced force in surrounding rock tends to a less value after tunnel excavation. And it does not consider the effect of actual time. The parameters in calculating unavoidably exist difference with the parameter of rock mass in reality. These reasons lead to the difference between the coupling analysis and the engineering measurement. But the results obtained in section 4.1 are less than the measuring results considering it indicates that the numerical analysis without underground water seepage flow cannot meet the need of engineering.

5 Conclusions

1) When underground water seepage flow function is considered in coupling fluid-mechanical analysis, the calculation vault settlements have finally achieved

5.7−6.0 mm with the interaction of underground water seepage flow and stress release in surrounding rock around the tunnel. The coupling calculation results are very close to the vault measurement settlement. It indicates that constructing tunnels in aquiferous stratum the underground water seepage flow effect must be considered in the design phase.

2) The settlement of the surrounding rock above the tunnel has close relationship with its own position. The region near the tunnel excavation zone has the biggest rock deformation, so it should promptly complete supporting measures. When not considering the seepage flow function, the farther the region, the smaller the rock deformation; but when considering the seepage flow function, the settlement of the surrounding rock is above the tunnel and then basically tends to stable in shallower tunnel and it has obviously influence on the ground surface subsidence.

References

[1] DANIELLE P, GERARD B, JEAN-PHILIPPE V. Injection of a ventilation tower of an underwater road tunnel using cement and chemical grouts[C]// Proceedings of the Third International Conference: Grouting and Ground Treatment. New Orleans, LA: The Geo-Institute of ASCE, 2003, 120(2): 1605−1616.

[2] TSENG D J, TSAI B R, CHANG L C. A case study on ground treatment for a rock tunnel with high groundwater ingression in Taiwan[J]. Tunneling and Underground Space Technology, 2001, 16(3): 175−183.

[3] ZHOU Chong, LUO Qiong, LI Zhi-guo, YANG Yong. Techniques for tackling lining cracks and leakages in Yuanliangshan tunnel[J]. Modern Tunnelling Technology, 2004, 41(5): 52−57. (in Chinese)

[4] LIU Xiao-bing, CHEN Yu. Structural calculation and analysis for double arch tunnel in water eroded groove[J]. J Cent South Univ: Science and Technology, 2005, 36(3): 517−521. (in Chinese)

[5] YANG Xiao-li, ZHANG Bing-qiang, WANG Zhi-bin, ZOU Jin-feng, LI Liang. Earthquake response of large span and double arch shallow tunnel[J]. J Cent South Univ: Science and Technology, 2006, 37(5): 991−996. (in Chinese)

[6] LI Ting-chun, LI Shu-cai, CHEN Wei-zhong, QIU Xiang-bo. Coupled fluid-mechanical analysis of Xiamen sub sea tunnel[J]. Chinese Journal of Geotechnical Engineering, 2004, 26(3): 397−401. (in Chinese)

[7] ZANGERL C, EBERHARDT E, LOEW S. Ground settlements above tunnels in fractured crystalline rock: Numerical analysis of coupled hydro mechanical mechanisms[J]. Hydrogeology Journal, 2003, 32(11): 162−173.

[8] LEE I M, NAM S W. The study of seepage forces on the tunnel lining and tunnel face in shallow tunnels[J]. Tunnelling and Underground Space Technology, 2001, 16(1): 31−40.

[9] LEE I M, NAM S W. Effect of tunnel advance rate on seepage forces acting on the underwater tunnel face[J]. Tunnelling and Underground Space Technology, 2004, 19(3): 273−281.

[10] YANG Hui-jun, WANG Meng-shu. Analysis on construction factors of surrounding rock deformation in tunneling works[J]. Journal of the China Railway Society, 2006, 28(3): 92−96. (in Chinese)

[11] TANG Jian-xin, CAI Shi-ming, LIU Hong-zhou, DAI Gao-fei. Analyses of rock mass displacement of Jinyun tunnel[J]. Journal of Chongqing University, 2002, 25(12): 137−140. (in Chinese)

[12] COULTER S, MARTIN C D. Effect of jet-grouting on surface settlements above the Aeschertunnel, Switzerland[J]. Tunnelling and Underground Space Technology, 2006, 21(5): 542−553.

[13] VILLY A, KONTOGIANNI T, STIROS S C. Induced deformation during tunnel excavation: Evidence from geodetic monitoring[J]. Engineering Geology, 2005, 79: 115−126.

[14] LI Di-yuan, LI Xi-bing, ZHANG Wei, GONG Feng-qiang, HUANG Bin-ren. Stability analysis for surrounding rock of multi-arch tunnel based on coupled fluid-mechanics theorem[J]. Chinese Journal of Rock Mechanics and Engineering, 2007, 26(5): 1056−1064. (in Chinese)

[15] JI Xiao-ming, WANG Yu-hui. Hydro mechanical coupling analysis of tunnel excavation process[J]. Chinese Journal of Underground Space and Engineering, 2005, 1(6): 848−852. (in Chinese)

[16] Itasca Consulting Group, Inc. FLAC^{3D} Fluid-mechanical interaction(Version 2.1)[R]. 2003.

(Edited by YANG Hua)